IWASE, M. Developments in zirconia sensors during the 1980's – Laboratory and in-plant applications in iron- and steelmaking. *INFACON 6. Proceedings of the 1st International Chromium Steel and Alloys Congress, Cape Town.* Volume 2. Johannesburg, SAIMM, 1992. pp. 49–61.

Developments in Zirconia Sensors during the 1980's—Laboratory and In-Plant Applications in Iron- and Steelmaking

M. IWASE

Kyoto University, Kyoto, Japan

Recent developments of solid-state sensors are discussed, with particular emphasis on *in situ* determinations of silicon, phosphorus, and chromium in liquid steel, as well as blast-furnace hot metal. During the last decade, a variety of applications of solid-state electrochemical sensors have become possible, also in laboratory applications. Recent developments in this field include (i) determinations of electronic conduction in zirconia electrolytes and (ii) activity determinations of FeO, P_2O_5, and Cr_2O_3 in molten slags. Solid-state sensors can also be applied in an automatic facility for the determination of FeO activities. This equipment enables the FeO activities to be determined within 3 to 5 minutes in laboratories. With this equipment, on-line determinations of FeO activities have now become possible in BOF melt shops.

Introduction

For many years control strategies in iron- and steelmaking processes depended on samples taken from molten steel, liquid slag, gas phase, and final products. Because of recent developments in the areas of dynamic control systems, however, there is a strong incentive to develop diagnostic sensors that will permit rapid determinations of various elements dissolved in hot metal and liquid steel[1]. Electrochemical sensors incorporating stabilized zirconia solid electrolytes would meet such requirements.

Stabilized zirconia is predominantly an oxygen anion conductor because of the presence of a large amount of oxygen anion vacancies. The open-circuit emf of the galvanic cell incorporating a zirconia electrolyte is a measure of the oxygen potential difference across the electrolyte:

$$E = \frac{RT}{4F} \ln \frac{P'_{O_2}}{P''_{O_2}}, \qquad [1]$$

where P'_{O_2} and P''_{O_2} are the oxygen partial pressures at the two electrodes respectively, and the other symbols have their usual meaning. However, with the incorporation of an appropriate auxiliary electrode or tri-phase zirconia electrolyte, the open-circuit cell potentials of zirconia sensors can provide a measure of the chemical potentials of elements other than oxygen.

The recent progress in control technologies also necessitated accelerated research activities in the thermodynamic study of iron- and steelmaking. The apparent advantage of solid-state zirconia sensors, even in laboratory experiments, would be that

- thermochemical properties in a variety of condensed phases can rapidly be determined,
- laboratory measurements can be extended to in-plant applications with minor modifications.

This paper is aimed at discussing recent developments in such zirconia sensors designed to measure chemical potentials of various species in liquid steel, hot metal, and molten slag for use in both laboratory and in-plant applications of iron- and steelmaking processes.

Oxygen Sensors

The importance of oxygen in iron- and steelmaking processes cannot be over emphasized. Deoxidation, reoxidation, dephosphorization, desulphurization, all are related to the oxygen potential in the various stages of steelmaking processes. The application of zirconia sensors to directly measure the oxygen activities in molten steel was initiated in the late 1960's[2]. The application of oxygen sensors in an industrial environment, however, has not been without problems. For example, Thomas reported, in 1975, that different oxygen sensors would yield different oxygen activities, even if the measurements were made in the same vessel[3]. These differences could be attributed to the fact that different oxygen sensors utilize different zirconia electrolytes. Hence the extent of electronic conduction is not the same in the various commercial oxygen sensors[4,5].

When a zirconia electrolyte exhibiting both ionic and *n*-type electronic conduction at low oxygen potentials and high temperatures is incorporated into an oxygen concentration cell, the electromotive force can be expressed as follows[6]:

$$E = \frac{RT}{F} \ln \frac{P'^{1/4}_{O_2} + P_\theta^{1/4}}{P''^{1/4}_{O_2} + P_\theta^{1/4}} , \qquad [2]$$

where P_θ is the oxygen partial pressure at which the n-type and ionic conductivities are equal. Under conditions where mixed ionic and n-type electronic conduction are prominent, a concentration gradient will result across the boundary layer between molten steel and zirconia because of the migration of oxygen anions through the electrolyte[6,7], and the resulting cell potential under these circumstances is given by[4,8]

$$E = \frac{RT}{F} \ln \frac{P'^{1/4}_{O_2} + P_\theta^{1/4}}{\{[\%\,O]_i / K\}^{-1/2} + P_\theta^{1/4}} , \qquad [3]$$

where K is the equilibrium constant for the dissolution of gaseous oxygen at unit atmospheric pressure into liquid iron at 1 wt per cent solution:

$$(1/2)\,O_2(g) = 0\ (\%, \text{in Fe}).$$

The oxygen concentration, in per cent by weight, in liquid steel at the liquid steel/zirconia electrolyte interface, $[\%O]_i$, is given by[9,10]

$$(RT\,\sigma_{ion}/2\,L)\,[\ln\{1 + P_\theta^{1/4}(K/[\%O]_i^{-1/2}\} - \ln\{1 + P_\theta^{1/4} P''^{1/4}_{O_2}\}] = (m\,d/1600)\,([\%O]_b - [\%O_i]) , \qquad [4]$$

where m is the mass transport coefficient for oxygen, d is the density of the liquid steel, σ_{ion} is the ionic conductivity, L is the wall thickness of the electrolyte, and $[\%O]_b$ is the oxygen concentration in the bulk of the molten steel. It should be emphasized that, for the control of the steelmaking process, a knowledge of $[\%O]_b$ rather than of $[\%O]_i$ is required.

From equation [4], values for $[\%O]_i$ can be computed as a function of $[\%O]_b$, and the relationship between the measured emf and $[\%O]_b$ is then obtained from equation [3]. The *emf*–$[\%O]_b$ relationship can be influenced significantly by

(i) the ionic conductivity, σ_{ion},

(ii) the parameter P_θ, and

(iii) the thickness, L, of the electrolyte.

Values for these parameters should remain constant for a specific commercial probe design. However, these parameters, especially P_θ, may vary from one commercial-grade zirconia to another. For this reason, concerted efforts were devoted in the 1980s to elucidate the extent of n-type electronic conduction in commercial-grade zirconia electrolytes.

In addition, the performance of electrochemical probes is strongly influenced by an unpredictable factor corresponding to the liquid-phase mass transport coefficient, m, for oxygen in liquid steel. This parameter depends markedly on the hydrodynamic condition of liquid steel, and hence will vary from one steelmaking vessel to another. From the foregoing comments it is very likely that even the same type of oxygen probe would indicate different oxygen activities when the measurements were conducted under different conditions or in different vessels. Indeed, such a problem has been encountered in steelmaking processes. This is shown in Figure 1[11]. Curve 1 indicates the relationship between oxygen concentrations determined by the electrochemical method in one steelmaking vessel and those obtained by chemical analysis; good agreement was obtained. However, when emf measurements were made in another vessel, the oxygen concentrations determined by the emf method were much lower than those obtained by chemical analysis, as indicated by the solid circles. Note that the two sets of measurements were made with the same type of commercial oxygen probe. The disagreement in measured oxygen concentrations between the two vessels was eliminated by taking into account the difference in oxygen concentration between the electrolyte/molten steel interface and the bulk of the liquid steel, and this is shown by the open circles in Figure 1.

By using the coulometric titration technique developed by Swinkels[12], the parameter P_θ has been measured by Janke[13], Iwase[14,15], and Dippenaar[16]. At present, values for this parameter for commercially available zirconia electrolytes have been well delineated, and these measurements have contributed significantly to the improvements in oxygen sensors. Because of these concerted efforts to elucidate the sources of errors associated with oxygen sensors during the 1980's, the application of oxygen probes is spreading throughout the world. In 1990, for example, the Japanese steel industry consumed 600 000 oxygen probes.

Measurement of Silicon

Silicon Levels in Hot Metal

In North America, the average silicon content of hot metal is about 1 wt per cent, while in Japan and Europe the average is between 0,4 and 0,7 wt per cent. In order to clarify the effect of silicon content on blast-furnace and BOF operations, Cosma and Strathdee[17] compared the energy input at the blast furnace to reduce SiO_2 and dissolve silicon in hot metal, with the energy output in the BOF as determined by the net gain in scrap-melting capacity. They concluded that the optimum silicon content of hot metal should be 0,7 wt per cent in North America. The optimum hot-metal silicon, however, depends on the ratio of hot metal to scrap in the BOF. This ratio is 92 to 97 per cent in Japan, and 70 to 85 per cent in North America.

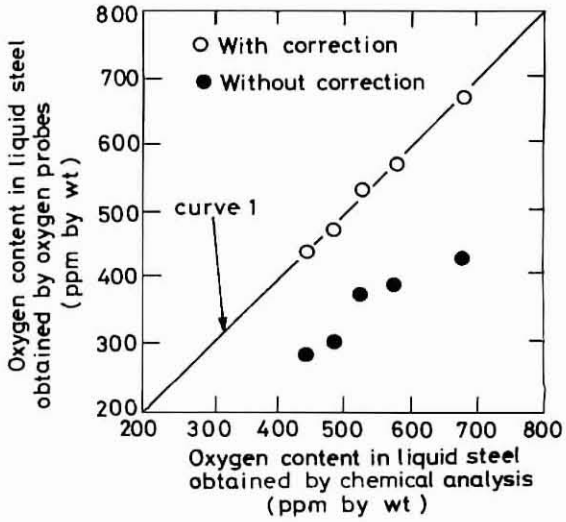

FIGURE 1. Relation between oxygen concentrations determined with oxygen sensors and by chemical analysis

This finding means that the optimum silicon content is 0,2 to 0,4 wt per cent for iron- and steelmaking operations in Japan[18].

The production of hot metal with a low silicon content can result in appreciable cost savings for the blast furnace as well as for the BOF process[19]. In order to take full advantages of using low-silicon hot metal in BOF steelmaking, increased attention is being directed towards an appropriate method for the external removal of silicon from the hot metal[19,20]. Such external desiliconization can be achieved by blowing nitrogen gas through a top-blowing lance while adding solid iron oxide through a charging chute. As an alternative, mill-scale and lime additions can be made without gas blowing, at the tilting spout or into the hot-metal runner. Regardless of the addition technique, the removal of silicon from hot metal can be represented by[18]

$$\ln \{[Si]_f / [Si]_i\} = - k W, \qquad [5]$$

where $[Si]_f$ is the final silicon content attained, $[Si]_i$ is the initial silicon content, W is the amount of flux consumed, and k is a constant. This equation shows that precise control of the final silicon content, $[Si]_f$, requires a knowledge of the initial silicon concentration, $[Si]_i$, so that appropriate additions of the flux can be made. The concentration of silicon in hot metal, however, varies significantly.

Figure 2(a) shows the variation of silicon levels of hot metal leaving the no. 4 blast furnace of Kimitsu Works, Nippon Steel Corporation[21]. This furnace is equipped with 4 tap holes and has an internal volume of approximately 5000 m^3. During the period between March 29, 1990, and April 4, 1990, the no. 4 blast furnace was under very stable operation. Nevertheless, as shown in this figure, variations in silicon levels of ±0,05 to ±0,10 wt per cent were experienced during a single tapping.

On April 22, 1990, the no. 4 furnace was taken out of blast to perform various maintenance functions for over 16 hours, while the subsequent blowing-in practice was started at 19:00 on April 23, 1990. At 23:00 on April 23, 1990, the first hot metal was tapped after the blowing-off practice. Figure 2(b) shows the variation of hot-metal silicon from April 23 to 24 after this scheduled maintenance. The variation of hot-metal silicon was up to ±0,3 wt per cent, and fairly large fluctuations of hot-metal silicon persisted for over 12 hours.

From the foregoing comments, it is evident that the key to better control of the silicon levels in hot metal through an external desiliconization process is the use of a sensing device that allows for the rapid determination of the silicon content.

Silicon Sensor Incorporating Auxiliary Electrode

Silicon sensors can be designed by the use of appropriate solid electrolytes. Ideally, a solid-state silicon probe requires a Si^{4+}-ion conductor as electrolyte. Despite the concerted effort of many laboratories during the last three decades to find a suitable Si^{4+}-ion conducting electrolyte, there are no candidate materials that have been identified as Si^{4+}-ion conductors. An alternative approach is to use a zirconia electrolyte in conjunction with an appropriate auxiliary electrode.

Iwase[21–23] has studied an electrochemical silicon sensor incorporating an auxiliary electrode of (ZrO_2 + $ZrSiO_4$) or (ZrO_2 + $ZrSiO_4$ + $Na_2ZrSi_2O_7$) mixture. The phase relations of the system (ZrO_2 + SiO_2 + Na_2O) in the vicinity of the ZrO_2 apex is shown in Figure 3[24]. Within the three-phase region (ZrO_2 + $ZrSiO_4$ + $Na_2Si_2ZrO_7$), the activity of SiO_2 is fixed by the reaction

$$ZrO_2 + SiO_2 \text{ (in auxiliary electrode)} = ZrSiO_2 . \qquad [6]$$

The SiO_2 activity fixed by the two-phase coexistence of ZrO_2 + $ZrSiO_4$ is identical to that by the three-phase region of ZrO_2 + $ZrSiO_4$ + $Na_4ZrSi_2O_7$. The silicon sensor can be expressed by

Mo / Mo + MoO_2 / ZrO_2(MgO) / (SiO_2)aux. /
Si(hot metal) / Fe .

The oxygen potential at the three-phase interface (electrolyte + molten iron + auxiliary electrode) is established by the equilibrium reaction

$$Si(\text{in Fe}) + O_2 = SiO_2(\text{in auxiliary electrode}) . \qquad [7]$$

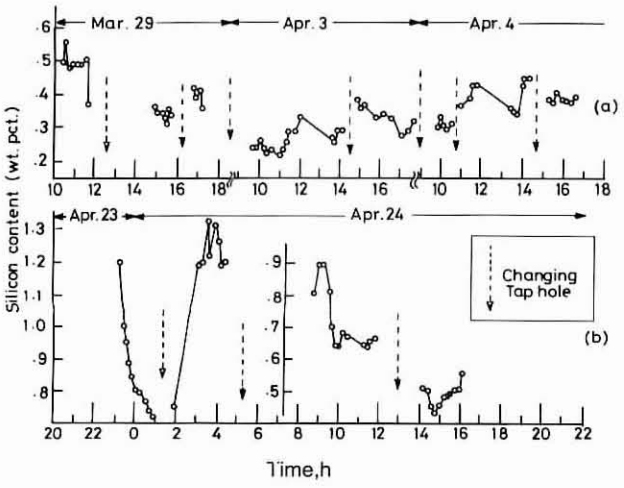

FIGURE 2. Variation of silicon levels in hot metal leaving no. 4 blast furnace at Kimitsu Works, Nippon Steel Corporation, (a) under stable blast furnace operation and (b) after scheduled maintenance

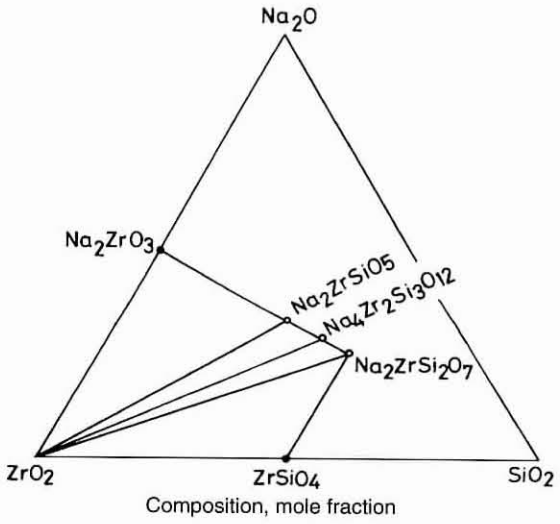

FIGURE 3. Phase relations in the system ZrO_2 + SiO_2 + Na_2O near the ZrO_2 apex at temperatures near 1723 K

It follows that

$$ZrO_2(s) + Si(\text{in Fe}) + O_2 = ZrSiO_4(s). \quad [8]$$

$$\log K(8) = -\log h_{Si} - \log P_{O_2}, \quad [9]$$

where h_{Si} is the activity of silicon in molten iron referred to 1 wt per cent solution. From equation [9] it follows that a measure of oxygen partial pressure, P_{O_2}, corresponds to a knowledge of the activity of silicon, h_{Si} The open-circuit cell potential is given by

$$E = \frac{RT}{F} \ln \frac{P'^{1/4}_{O_2} + P^{1/4}_{\theta}}{\{K(8)_i h_{Si}\}^{-1/4} + P^{1/4}_{\theta}} . \quad [10]$$

A schematic diagram of the silicon sensor, Mo/Mo + $MoO_2/ZrO_2(MgO)/(SiO_2)$aux, is given in Figure 4. The cell consists of an MgO-stabilized zirconia tube incorporating the auxiliary electrode and the reference electrode (Mo + MoO_2).

For the preparation of the auxiliary electrode, the magnesia-stabilized zirconia tube was first painted with a slurry of either (ZrO_2 + $ZrSiO_4$) or (ZrO_2 + $ZrSiO_4$ + $Na_2Si_2ZrO_7$) mixture: blobs of 2 to 3 mm diameter and 0,5 to 1,0 mm thickness were formed on the outer surface of the tube, which was dried at ambient temperature and subsequently sintered at 1723 K for 20 minutes. Better adhesion was obtained with a mixture of (ZrO_2 + $ZrSiO_4$ + $Na_2Si_2ZrO_7$) than with (ZrO_2 + $ZrSiO_4$).

The silicon sensor was first evaluated in experiments using small crucibles with 5 kg of {Fe + Si + C} alloys at 1773 K and 1823 K respectively. In Figure 5, measured cell potentials at 1773 K and 1823 K respectively are shown as a function of silicon activities, h_{Si}, in {Fe + C + Si} melts.

Various designs of the auxiliary electrode, (ZrO_2 + ZrSiO4), were studied in great detail by Janke *et al.*[25], Figure 6, and it was shown that the cell designs designated C and D showed satisfactory cell performance.

The silicon sensor was also evaluated by conducting in-plant measurements in the hot-metal runner of no. 4 blast furnace of Kimitsu Works, Nippon Steel Corporation[21]. In contrast to {Fe + Si + C} alloys used in the crucible experiments, practical blast-furnace hot metal contains a variety of elements, i.e. C, Si, Mn, P, S, Cr, Ni, Cu, Ti. For the calculation of the activity, h_{Si}, in hot metal, it is therefore imperative that chemical analyses be obtained for at least C, Si, Mn, P, and S in order to calculate the silicon activity accurately. In addition, the hot-metal temperature changes very significantly even during tapping; see Figure 7. For this reason, it is not possible to use an isothermal plot of measured cell potentials against the silicon activity. However, for the control of silicon levels in hot metal, a knowledge of the silicon concentration rather than the silicon activity is required, and it is preferable to derive a regression formula based on the results of in-plant tests.

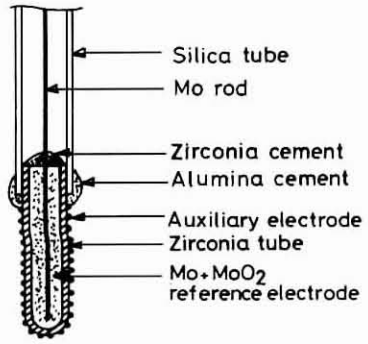

FIGURE 4. Schematic diagram of a silicon sensor incorporating an auxiliary electrode of ZrO_2 + $ZrSiO_4$ + $Na_2Si_2ZrO_7$ or ZrO_2 + $ZrSiO_4$

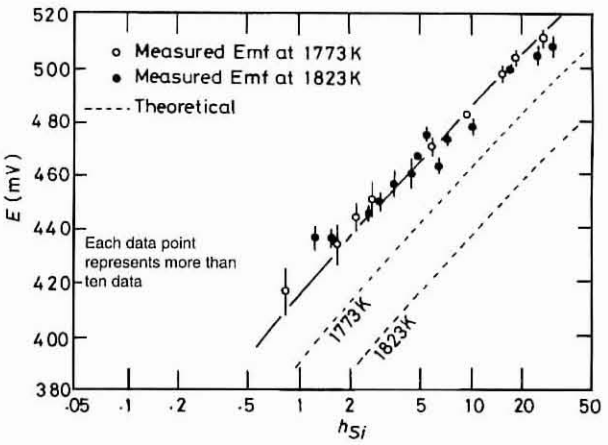

FIGURE 5. Semi-logarithmic plot of the cell potentials of the silicon sensor Mo / Mo +MoO_2 // $ZrO_2(MgO)$ // ZrO_2 + $ZrSiO_4$ + $Na_2Si_2ZrO_7$, and silicon concentration in percentages by weight at 1773 K and 1823 K

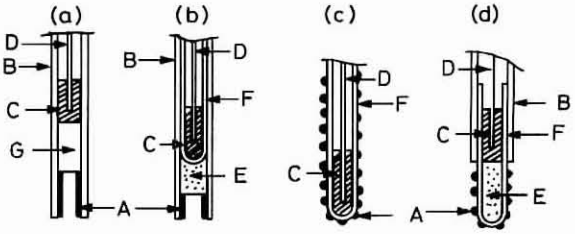

A. ZrO_2 + $ZrSiO_4$, B. alumina tube, C. Cr + Cr_2O_3, D. Ir wire, E. $ZrO_2(Y_2O_3)$ powder, F. zirconia tube, G. zirconia plug

FIGURE 6. Various designs for the auxiliary electrode ZrO_2 + $ZrSiO_4$ after Raiber, Tu, and Janke[25]

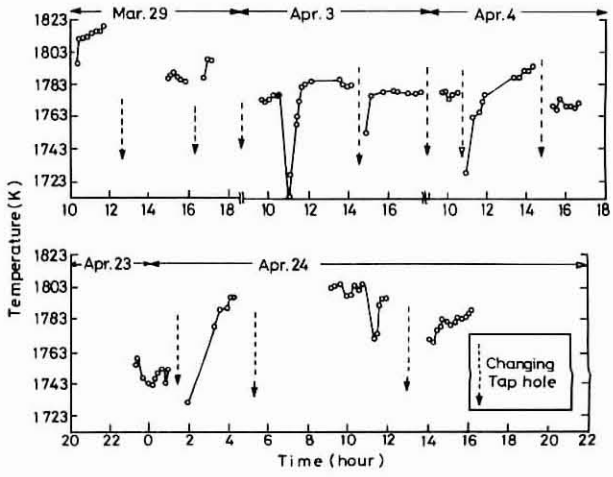

FIGURE 7. Variation in the temperature of hot metal leaving no. 4 blast furnace at Kimitsu Works, Nippon Steel Corporation, during a period between March 29 and April 24, 1990

Equation [10] shows that the silicon concentration in per cent by wt, *[%Si]*, is given by

$$[\%Si] = \exp\{L_O + L_1(E/T) + L_2/T\} / f_{Si}, \quad [11]$$

where L_0, L_1, and L_2 denote constants. The activity coefficient, f_{Si}, depends on the temperature and the concentrations of Si and other elements dissolved in the hot metal. Nevertheless, for industrial application of silicon sensors, values for f_{Si} can be estimated and, although there is no theoretical formula that can express analytically f_{Si} as a function of E and T, a first approximation yields

$$f_{Si} = \exp(L_4 + L_5 E + L_6 T). \quad [12]$$

By combining equations [11] and [12],

$$[\%Si] = \exp\{C_0 + C_1E + C_2(E/T) + C_3T + C_4/T\}, \quad [13]$$

where C_0, C_1, C_2, C_3, C_4 are constants and these were obtained by using the experimental results of in-plant tests.

Figure 8 compares the silicon content, as determined by chemical analysis, $[\%Si]_{analysis}$, with those measured by silicon sensors, $[\%Si]_{emf}$; a standard deviation (one sigma) of ±0,06 per cent and a correlation factor (r) of 0,85 were obtained.

Silicon Sensor Based on Tri-phase Zirconia Electrolyte

The preparation of the auxiliary electrode, (ZrO_2 + $ZrSiO_4$) or (ZrO_2 + $ZrSiO_4$ + $Na_2ZrSi_2O_7$) mixture, is labour-intensive and time-consuming. As an alternative approach, Iwase[26] proposed the use of a tri-phase zirconia electrolyte, which consists of a cubic ZrO_2–MgO solid solution, monoclinic ZrO_2, and $2MgO.SiO_2$ for the rapid measurements of silicon potentials in hot metal.

Figure 9 shows the isothermal section of the phase diagram for the system (ZrO_2 + MgO + SiO_2)[26]. The solid circle indicates the composition of the tri-phase zirconia electrolyte: the electrolyte composition lies in the three-phase region of the cubic ZrO_2–MgO solid solution, tetragonal ZrO_2, and forsterite, $2MgO.SiO_2$.

Figure 10 shows a collection of microprobe analyses of the tri-phase electrolyte. It is known that silica contained in magnesia-stabilized zirconia is found as a second phase, i.e. $2MgO.SiO_2$, at the grain boundaries[27]. Such a second phase is indeed observed as shown in Figure 10(a); the magnesium and silicon contents are higher at the grain boundaries than in the grains, corresponding to the formation of $2MgO.SiO_2$, Figures 10(b) and (c).

The silicon sensor incorporating a tri-phase zirconia electrolyte can be expressed as

Mo / Mo + MoO_2 / tri-phase zirconia electrolyte / Si (in Fe).

When a tri-phase zirconia electrolyte is in contact with molten iron containing silicon, the following equilibrium will be established at the electrolyte/molten iron interface;

$$2\,MgO(\text{in } ZrO_2) + Si(\text{in Fe}) + O_2(\text{in Fe}) = 2MgO.SiO_2 . \quad [14]$$

$$\log K(14) = -2\log a_{MgO} - \log h_{Si} - \log P_{O_2}, \quad [15]$$

where a_{MgO} is the activity of MgO within the tri-phase zirconia: at any given temperature the activity of MgO within the electrolyte is fixed. From equation [15], it appears that a measure of the oxygen partial pressure, P_{O_2}, corresponds to a knowledge of the activity of silicon.

Figure 11 shows the relationship between the measured cell potential and the activity of silicon at 1723 K, obtained by laboratory experiments with 600 g of {F + C + Si} alloys; open-circuit emf's show satisfactory sensitivity to variations of the silicon activity.

The silicon sensor based on a tri-phase zirconia electrolyte was also evaluated by conducting in-plant measurements. Figure 12 shows the relationship between the silicon content as measured with a tri-phase silicon sensor, $[\%Si]_{emf}$, and that determined by chemical analysis, $[\%Si]_{analysis}$.

The use of a tri-phase zirconia solid electrolyte is advantageous because the manufacturing procedure for this electrolyte is very similar to that for conventional zirconia tubes, and commercial production facilities for zirconia ceramics can easily be converted to the fabrication of the tri-phase zirconia electrolyte.

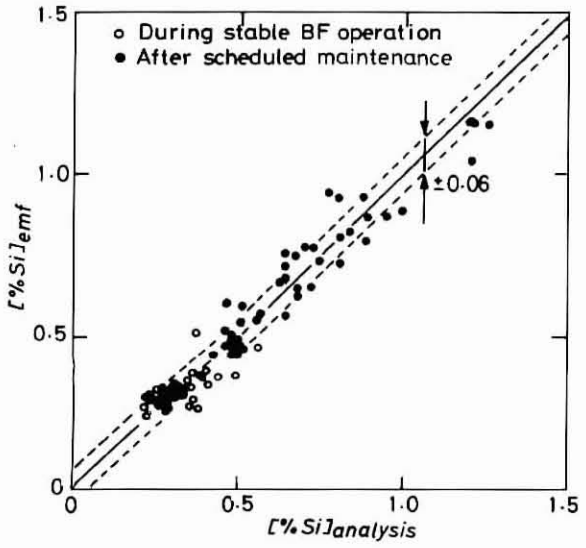

FIGURE 8. Silicon concentrations determined with silicon sensors incorporating an auxiliary electrode, $[\%Si]_{emf}$, as a function of those determined by chemical analysis, $[\%Si]_{analysis}$

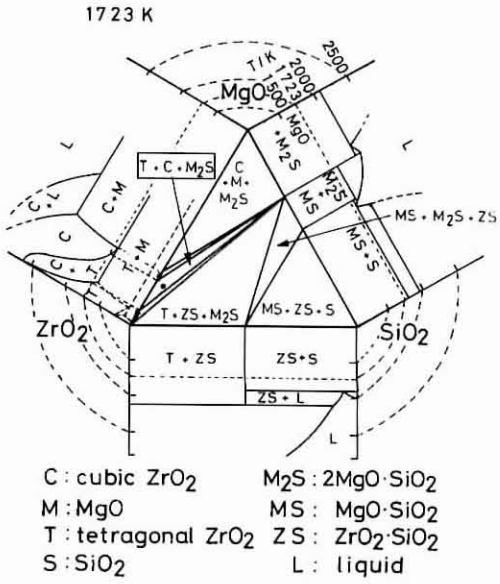

FIGURE 9. Phase relations in the system ZrO_2 + MgO + SiO_2 at temperatures near 1723 K

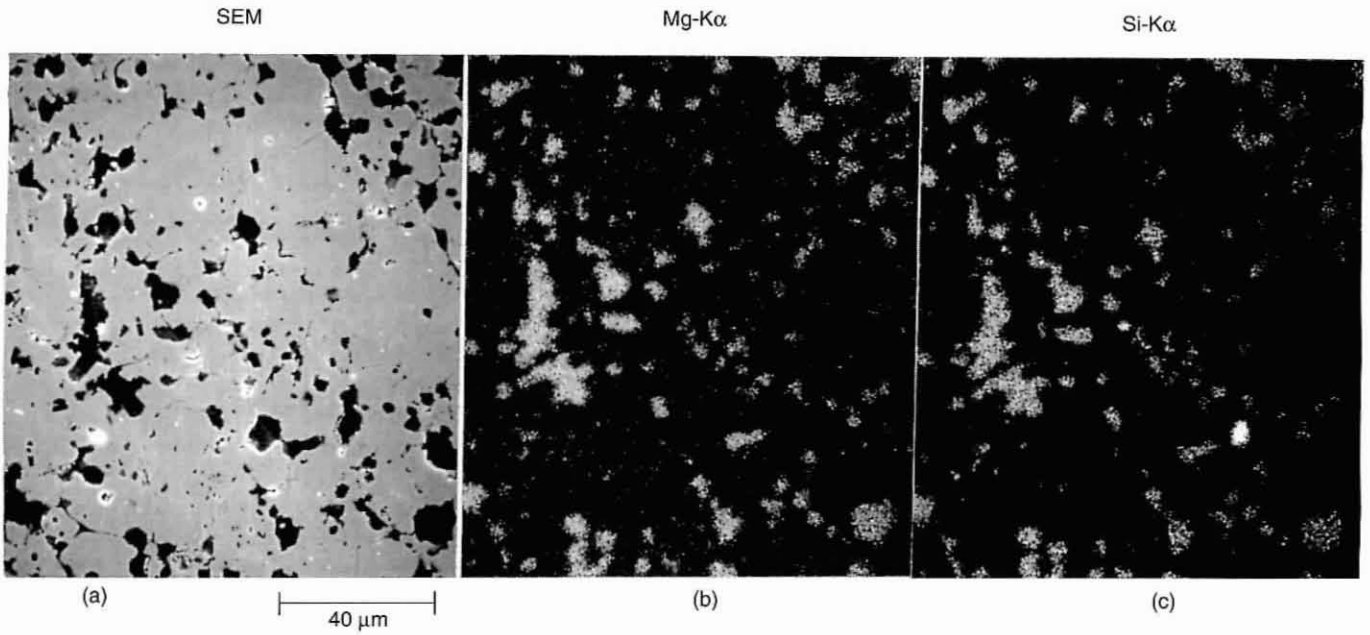

FIGURE 10. Collection of microprobe analyses of the tri-phase zirconia electrolyte

Oxygen Sensor for Measuring Silicon in Hot Metal

In some instances, particularly in North America, the hot metal may already be in equilibrium with SiO_2, which would be present as a very thin film on the hot-metal surface or as fine particles within the hot-metal[20]:

Si(in the hot metal) + 2 O(in the hot metal) =
SiO_2(on the surface of the hot metal) . [16]

Reaction [16] is exothermic; therefore the possibility of 'self equilibrium' would increase with a decrease in hot-metal temperature. The presence of a thin film of silica on cast iron is well known and can be observed by the naked eye. Indeed, in some foundries, pouring temperatures are judged by the presence of a silica film since, at temperatures higher than 1723 K, the silica film is reduced by carbon:

SiO_2(in cast iron) + 2 C(in cast iron) =
Si(in cast iron) + 2 CO . [17]

In North America, the temperature of the hot metal leaving the blast furnace is usually below 1723 K. If equilibrium with respect to silica is attained within the hot metal, then a measure of the oxygen potential, which can be obtained by the conventional oxygen probe, will be directly related to the silicon content of the hot metal. Consequently, it is possible to use the conventional oxygen sensor in the North American steel industry for the determination of silicon in the hot metal when the silicon levels are higher than 0,7 per cent and the temperature is below 1723 K.

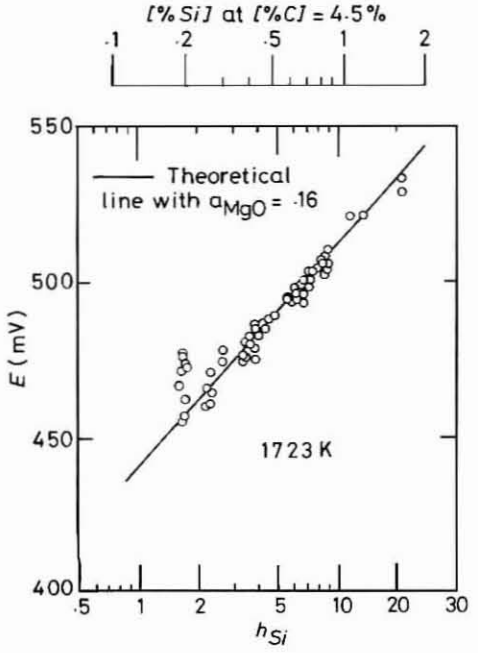

FIGURE 11. Semi-logarithmic plot between measured cell potentials of the silicon sensor Mo / Mo + MoO_2 / tri-phase zirconia electrolyte and the activity of silicon

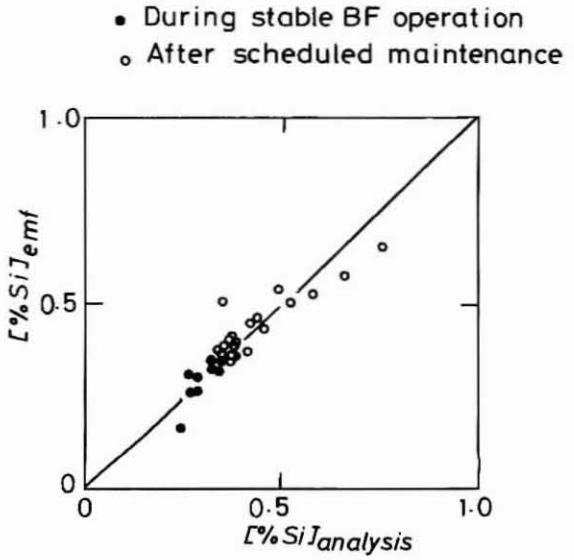

FIGURE 12. Relation between silicon concentrations determined with a tri-phase silicon sensor, $[\%Si]_{emf}$, and those by chemical analysis, $[\%Si]_{analysis}$

Silicon Sensor Based on a Liquid Electrolyte

Although a relatively long response time (>40 to 120 seconds) is required, a silicon sensor can also be designed by using liquid silicates. Figure 13 shows schematically the cell designs used by Onouye *et al.*[28], Ichihara *et al.*[29], and Buiarelli and Granati[30].

In 1984, Onouye *et al.*[28] reported the use of {CaO + MgO + SiO_2 + CaF_2} liquid slags as electrolytes at 1773 K:

C / Si / {CaO MgO + SiO_2 + CaF_2}(l) / carbon-saturated (Fe + C + Si} / C.

A liquid electrolyte was maintained at the end of a silica tube. The electrolyte compositions were within a homogeneous liquid region, while the liquid electrolyte was in contact with pure SiO_2(s). A concentration gradient is established across the electrolyte during emf measurements.

Ichihara *et al.*[29] used a {CaO+ Al_2O_3 + SiO_2} slag saturated with solid SiO_2 as a liquid electrolyte at 1673 K:

Ni/ <Ni + Si>(s) + {Ni + Si}(l) / {CaO + SiO_2 + Al_2O_3}(l) + SiO_2(s) / {Fe + C + Si}(l),

while { CaO + MgO + SiO_2} slags saturated with solid SiO_2 were applied by Buiarelli and Granati[30] at 1773 K.

Although the cells performed well, as shown in Figure 14, in the experiments conducted by Ichihara *et al.* and Buiarelli and Granati, the compositions of the silicate electrolyte were within two-phase regions of SiO_2(s) + liquid slag, corresponding to a_{SiO_2} = 1. However, the activities of CaO and Al_2O_3 were not fixed within the liquid electrolyte, and concentration gradients of CaO and Al_2O_3 were established across the electrolyte. Hence, Ca^{2+} ions could migrate from one electrode to the other, resulting in diffusion potentials if emf measurements were made at temperatures other than their experimental temperatures. In addition, the construction of their silicon sensor requires fairly complicated procedures.

Chromium Sensor

In the production of stainless steel, close control of chromium levels in the molten steel is of crucial importance from the standpoint of better chromium recovery, metal yield, alloy additions, deoxidation, and final product quality. Electrochemical chromium sensors would consequently be of great assistance to ensure better control of the chromium levels. Figure 15 shows the construction of cells for this purpose, previously reported in the literature[31-34].

In 1988, Heinz and Janke[31] used a zirconia sensor incorporating Cr_2O_3 as auxiliary electrode:

Pt-Ph / Ir / Cr + Cr_2O_3 / ZrO_2(CaO) / Cr_2O_3 / {Fe + Cr}.

A small volume of liquid metal is allowed to fill a cavity at the sensor tip, to bring the liquid steel into equilibrium with Cr_2O_3, Figure 15(a):

2 Cr(in Fe) + (3/2) O_2 = Cr_2O_3 (in auxiliary electrode).

With this cell design, however, 30 seconds were required to obtain stable cell potentials after immersion in liquid steel, and this response time is evidently not short enough. In addition, the activities of chromium determined by this chromium sensor were much lower than those reported by Fruehan[32].

In order to develop a chromium sensor based on the use of an auxiliary electrode, a collaborative research programme was initiated in Japan by the Chromium Sensor Research

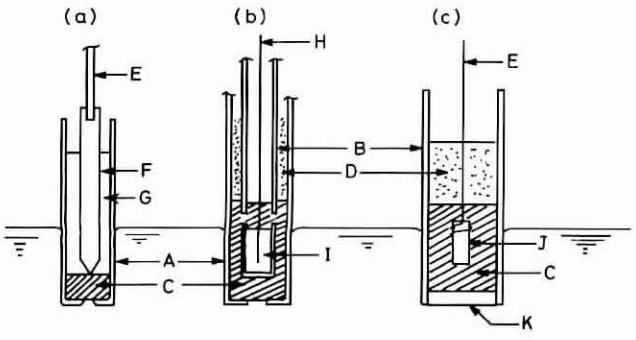

FIGURE 13. Cell designs of silicon sensors incorporating liquid-silicate electrolytes used by (a) Onouye *et al.*[28], (b) Ichihara *et al.*[29], and (c) Buiarelli and Granati[30]

A silica tube, B silica tube, C silicate electrolyte, D silica powder, E molybdenum wire, F graphite rod, G silicon powder, H nickel wire, I Ni(s) + {Ni–Si} (1) electrode, J Mo + Mo_3Si electrode, K porous silica

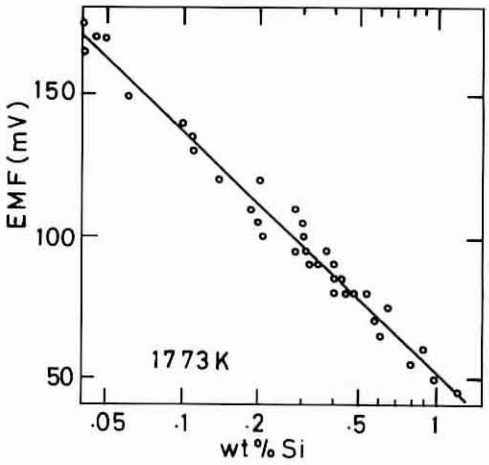

FIGURE 14. Relation between cell potential and silicon content obtained with a liquid-silicate electrolyte sensor[30]

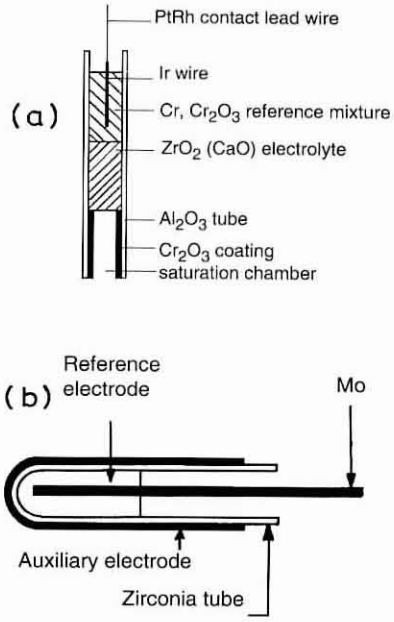

FIGURE 15. Cell constructions of chromium sensors (a) after Heinz and Janke, (b) after Iwase *et al.*[35]

Group of the Sensor Sub-Committee of the Steelmaking Committee of the Japanese Society for Promotion of Science (JSPS), under guidance of the author during the period between 1987 and 1990[32-34]. In addition to six university professors, the members included 38 representatives from the steel industry, ceramic companies and sensor manufacturers.

Various cell designs were evaluated through the collaborative research activities of JSPS as summarized in Table I, while a representative cell design is given in Figure 15(b). This cell consisted of a magnesia-stabilized zirconia tube incorporating an auxiliary electrode, a reference electrode, and a molybdenum rod as the electrical contact. Very good cell performance was obtained with this sensor, designated as 'KO' in Table I. With this sensor, the auxiliary electrode consisted of an equimolar mixture of (Cr_2O_3 + CaO + SiO_2). For the preparation of the auxiliary electrode, the outer surface of the zirconia tube was painted with slurry of the (CaO + SiO_2 + Cr_2O_3) mixture, heated to 1673 K for 20 minutes, and quenched.

According to the available phase diagram for the system (CaO + SiO_2 + Cr_2O_3)[35], the composition of the mixture is in a two-phase region of

Cr_2O_3(s) + {CaO + SiO_2 + Cr_2O_3}liquid slag

at 1873 K, corresponding to unit activity of Cr_2O_3 at the experimental temperature. Upon immersion in {Fe + Cr + C} alloys ([C] + 0,04 to 0,28 wt per cent), the cell potentials showed stable plateaus within 3 to 5 seconds and remained constant for more than 30 minutes. Figure 16 shows measured cell potentials with this 'KO' type of sensor as a function of the concentration of chromium in per cent by weight, [%Cr]. The measured emf's showed very good reproducibility (±1 mV).

In an alternative cell design, 'NO', of Table I, the auxiliary electrode consisted of 80 Cr_2O_3(s) + 10 CaF_2 + 10 $Al_6Si_4O_{13}$(mullite); compositions are given in per cent by weight. For the preparation of this auxiliary electrode, the zirconia tube was first dipped into a slurry of the auxiliary electrode, and then dried at ambient temperature. The phase relations of the system (Cr_2O_3 + CaF_2 + Al_2O_3 + SiO_2) are not known, but the binary phase diagram for the system (Cr_2O_3 + CaF_2) reveals the coexistence of the two phases Cr_2O_3(s) + {Cr_2O_3 + CaF_2}(l) in the slag. It can therefore be assumed that $Al_6Si_4O_{13}$ may act as an insulator or inert component within the auxiliary electrode. Indeed, the cell potentials obtained with the 'NO' sensor are very close to the theoretical line corresponding to $a_{Cr_2O_3}$ = 1, Figure 17.

Chromium sensors were also used by Geldenhuis and Dippenaar[36] for precise determinations of the activities of chromium in {Fe + Cr} alloys. In their measurements, {Fe + Cr}alloys were melted in an alumina crucible, the inside of which was coated with a layer of pure Cr_2O_3(s), and the equilibrium oxygen partial pressures were measured by zirconia sensors. In addition, great care was taken to ensure that equilibrium between the {Fe + Cr} alloys and the Cr_2O_3 was attained; the {Fe + Cr} melts were stirred for 40 minutes before emf measurements were made. The experimental results of Geldenhuis and Dippenaar at 1873 K are compared to those of the Japanese collaborative efforts in Figure 17, and very good agreement is found.

Phosphorus Sensor

In Japan, considerable attention has been focused on the removal of phosphorus from hot metal, a practice commonly referred to as external dephosphorization, for the reasons outlined below. In recent years, Japanese iron- and steelmakers have been obliged to significantly reduce steel production because of the unfavourable economic climate. For example, during the period between 1982 and 1985, 30 to 40 per cent of the Japanese blast furnaces had to be shut down. Also, the ratio of hot metal to scrap in the basic oxygen furnace has been markedly increased, resulting in a significant increase in hot-metal temperatures; as mentioned earlier, typical hot-metal temperatures are approximately 100 K higher in Japan than in North America. In addition, the Japanese steelmaking practice of lowering the slag volume, which is due in part to the efforts aimed at improving environmental control, tends to impair the removal of phosphorus. The average phosphorus content of hot metal from blast-furnaces in Japan is between 0,1 and 0,13 per cent, compared with that in North America of 0,08 to 0,107 per cent. These higher

TABLE I
CHEMICAL COMPOSITIONS OF ZIRCONIA ELECTROLYTES AND AUXILIARY ELECTRODES

Code name	Composition of zirconia	Composition of auxiliary electrode, mol%							Reference electrode
		Cr_2O_3	SiO_2	CaO	TiO_2	CaF_2	Mullite	ZrO_2	
K0	7 mol% MgO	33,3	33,3	33,3	–	–	–	–	Mo+MoO_2
N0	8 mol% MgO	80	–	–	–	10	10	–	Cr + Cr_2O_3
S0	9 mol% MgO	90	–	–	–	10	–	–	Cr + Cr_2O_3
O0	9 mol% MgO	75	10	–	–	15	–	–	Cr + Cr_2O_3
O1	9 mol% MgO	85	10	–	–	5	–	–	Cr + Cr_2O_3
O2	9 mol% MgO	75	20	–	–	5	–	–	Cr + Cr_2O_3
O3	9 mol% MgO	50 to 93	3 to 45	–	–	5 to 15	–	–	Cr + Cr_2O_3
Y0	9 mol% MgO	97	–	–	3	–	–	50	Mo+MoO_2
R0	8 mol% MgO	50	–	–	–	–	–	50	Cr + Cr_2O_3
E0	8 mol% Y_2O_3	100	–	–	–	–	–	–	Cr + Cr_2O_3
E1	8 mol% Y_2O_3	100	–	–	–	–	–	–	Cr + Cr_2O_3

phosphorus levels are due to the fact that the blast furnace operators in Japan rely on supplies of Australian iron ore, which has a relatively high phosphorus content.

Another factor in favour of the external dephosphorization of hot metal arises from the mixed top- and bottom-blowing techniques employed in pneumatic steelmaking. In these processes, oxygen is partially injected into the molten iron through submerged tuyères. In such combined top- and bottom-oxygen blowing, it is highly advantageous to minimize the charging time for molten metal, in order to protect the submerged tuyères. If the concentration of dissolved elements, especially phosphorus, can be lowered sufficiently by the external hot-metal treatment, the vessel can be tapped immediately after the termination of oxygen blowing. Such a practice can contribute significantly to the life of the submerged tuyères.

For the control of phosphorus levels in hot metal, a phosphorus sensor would be highly desirable. Iwase[37] has introduced a phosphorus sensor based on a three-phase zirconia electrolyte, which consists of ZrO_2–CaO solid solution + tetragonal ZrO_2 + $3CaO.P_2O_5$[38].
The electrochemical cell may be expressed as

Mo / Mo + MoO_2 / tri-phase electrolyte (fixed $a_{p_2O_5}$) /{Fe + C + P} / Fe.

Upon immersion in molten iron, equilibrium is established at the phase boundary between the tri-phase electrolyte and the metal:

2 P (in Fe) + 5 O(in Fe) = P_2O_5(in electrolyte).

The activity of P_2O_5 is fixed within the electrolyte in the same way as the activity of silica was fixed in the tri-phase electrolyte for silicon determinations.

Figure 18 shows the experimentally determined relationship between the cell potential and the phosphorus activity in a molten Fe–C–P-alloy at 1450°C.

FeO Sensor

Laboratory Applications

The study of the chemical reactions occurring in liquid steel and molten slags involves a complex slag system of at least eight important components, i.e. CaO, MgO, MnO, FeO, SiO_2, Al_2O_3, P_2O_5, CaF_2, and often a number of others such as Na_2O, TiO_2, Cr_2O_3, CaS. One of the greatest obstacles to the application of physico-chemical principles to the elucidation of slag–metal and slag–gas reactions is a lack of knowledge of the activities of the reacting species. Since iron oxide in slag participates in numerous reactions between the metal, slag, and gas, the evaluation of the activity of ferrous oxide should receive high priority.

Since the 1940's, a number of experimental determinations of the activities of ferrous oxide have been conducted[39]. Our knowledge of the activity of FeO is, nevertheless, still far from satisfactory. For example, consider a slag with the following composition: 40 CaO, 10 MgO, 5 MnO, 15 SiO_2, 10 Al_2O_3, 3 P_2O_5, 5 CaF_2, and 12 FeO, concentrations in per cent by weight. Data in the literature obtained in the course of half a century do not even allow the evaluation of a_{FeO} in this slag, and the experimental determination of the FeO activity is still required. However, if the activity of FeO in eight-component slags is required over a range of compositions, activity measurements must be conducted until millions of data points are obtained. Even if the activity determinations were focused on slags of high basicity, e.g. $X_{CaO} / X_{SiO_2} > 2$, a hundred thousand data points for a_{FeO} would be required. This is clearly an unrealistic task. Moreover, high-temperature experiments are time-consuming, and a lot of difficulties are encountered in such experiments. However, the zirconia sensor can be used for the rapid determination of the activity of FeO. Figure 19 shows the experimental set-up used for rapid determinations of the FeO activities in molten slags[40]. The technique consists essentially of charging the slag into an iron crucible together with pure silver to bring the molten slag into equilibrium with the solid iron crucible. The equilibrium oxygen partial pressure is then determined by means of a solid-state zirconia sensor.

The chemical potential of oxygen at the slag electrode is established by the reaction

Fe(s) + (1/2) O_2(g) = FeO(in slag). [18]

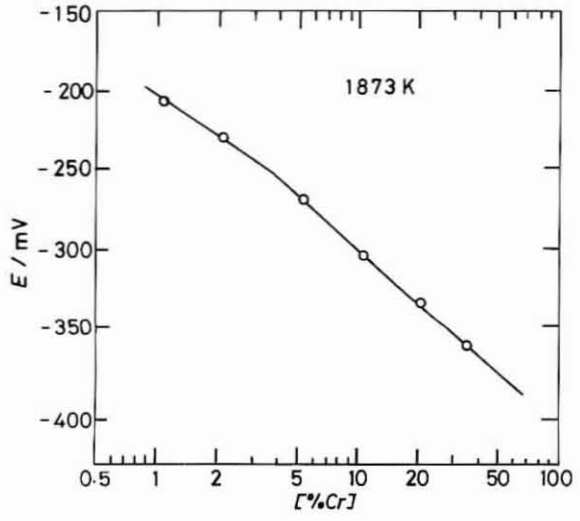

FIGURE 16. Relationship between the cell potential of chromium sensor KO of Table I and the chromium concentration in liquid iron at 1873 K[35]

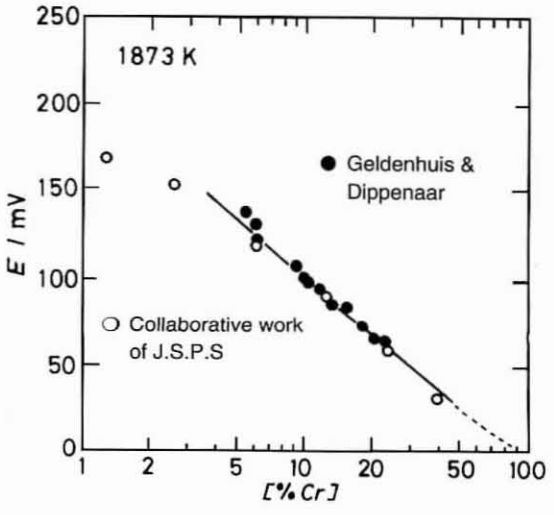

FIGURE 17. Relationship between the cell potential of chromium sensor NO of Table I and the chromium concentration[35], in comparison with the results of Geldenhuis and Dippenaar[36]

The activities of FeO can be calculated by

$$a_{FeO} = \left(\frac{P_{O_2}\ (slag)}{P^{\circ}_{O_2}\ (slag)} \right)^{1/2}, \qquad [19]$$

where $P^{\circ}_{O_2}(slag)$ is the equilibrium oxygen partial pressure of the mixture, 'pure' FeO(l) + Fe(s). The standard state for a_{FeO} is taken as 'pure' non-stoichiometric liquid FeO in equilibrium with pure solid iron.

Figure 20 shows the activities of FeO for the system (CaO + CaF_2 + SiO_2 + FeO) slags at 1673 K determined by Iwase *et al.*[41] (solid circles) and Van Wijngaarden and Dippenaar[42] (open circles). As shown in this figure, the two sets of experimental data are consistent with each other. Because of the many experimental difficulties in the determination of the activities in slags at high temperature, it is unlikely that such a good agreement would be obtained with other experimental techniques. The use of this FeO sensor was extended to 'on floor' activity determinations as mentioned in the foregoing section[43].

Automatic Activity Sensor for FeO

Traditionally, the presence of many of the large objectionable oxide inclusions in steel have been attributed to deoxidation practices, and much thought and effort have been devoted to the modification of deoxidation practices specifically to control the type and distribution of non-metallic inclusions. At present, with the increased use of argon rinsing, the size of the oxide inclusions that remain dispersed in the metal at the time of teeming are less than approximately 5 μm in diameter. Following the argon rinse, the total concentration of oxygen in aluminium-killed steel should be <20 p.p.m., corresponding to alumina inclusions of about 0,01 volume per cent[44].

However, in continuous-casting or ingot-making practices, inclusions of 50 to 100 μm in size (0,1 to 0,3 volume per cent) are not unusual. In 1970, Farrell, Bilek, and Hilty[45] showed that the presence of these large inclusions is primarily due to reoxidation of the molten-metal stream during teeming and/or poor practice of mould additions because the molten steel is inevitably brought into direct and/or indirect contact with air. An uncovered bath, a molten stream, or a mould cavity provides ample opportunity for liquid steel to react with the oxygen in the air. An obvious solution to reoxidation is to eliminate open-stream pouring between ladle-to-tundish and tundish-to-ladle by the use of submerged-entry nozzles. Recent developments in shrouding technology in continuous-casting practice are well covered by Harry[46].

Even when shrouding is employed, reoxidation can still occur when the molten steel is contained in a ladle. The reoxidation of aluminium by ferrous oxide in molten slags may be considered as follows:

$$2\ Al(in\ Fe) + 3\ FeO(in\ slag) = Al_2O_3 + 2\ Fe. \qquad [20]$$

Reaction [20] will proceed to the right-hand side with an increase in the FeO activity in the molten slag, with the result that much attention has been focused on the development of an appropriate practice aimed at lowering the FeO activity in molten slags, especially in secondary refining vessels. Currently, control strategies for lowering the FeO activities are based on samples taken from molten

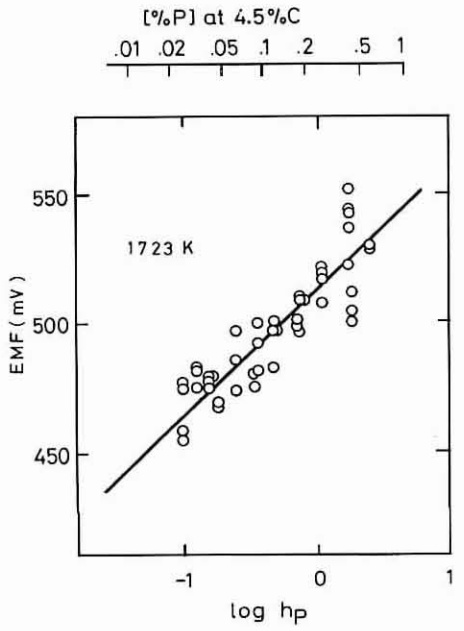

FIGURE 18. Relationship between the cell potential of a tri-phase phosphorus sensor and the phosphorus activity in liquid iron

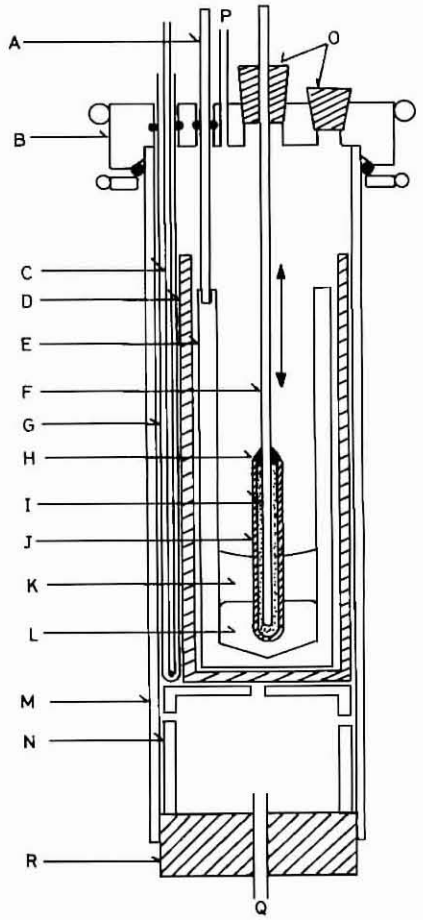

FIGURE 19. Experimental set-up for measurements of FeO activity

A steel rod, B water-cooled brass flange, C mullite sheath, D mullite crucible, E iron crucible, F molybdenum rod, G Pt–PtRh13 thermocouple, H zirconia cement, I Mo + MoO_2 reference electrode, J MgO-stabilized zirconia tube, K liquid slag, L liquid silver, M mullite reaction tube, N magnesia pedestal, O rubber stopper, P Argon outlet, Q Argon inlet, R rubber stopper

slags during ladle treatment. Based on practical experience, ladle-shop operators pay attention to the concentrations of 'total' Fe plus MnO, *(%T.Fe) + (%MnO)*. Manganese oxide can also re-oxidize aluminium, although *(%MnO) < (%T.Fe)*. However, chemical analyses of FeO and MnO in slags require at least 20 minutes, while the ladle treatment must be completed within 15 to 20 minutes. Hence, a knowledge of *(%T.Fe) + (%MnO)* based on chemical analysis cannot assist ladle-shop operators in the control of the molten slag during their operations.

The key to better control of FeO levels in molten slags would be the use of an electrochemical sensor that determines the FeO activity rapidly. However, in the case of slag an obvious drawback of solid-state sensors arises from the fact that the refractory component of the sensor would readily be attacked by the molten slag. In addition, owing to less slag in the ladle (less than 20 kg/t of steel) than in the BOF, it is extremely difficult to immerse a sensor in the slag only. For these reasons, Iwase developed an 'on floor' activity sensor for FeO. This equipment is based on samples taken from the slag. However, activity measurements can be completed within 5 minutes. A schematic illustration of the automatic activity sensor is shown in Figure 21. The electrochemical cell consists of a zirconia tube D (3,6 mm o.d., 2,2 mm i.d., and 32 mm in length), a (Mo + MoO_2) mixture C, and a molybdenum rod A of 1 mm diameter and 200 mm length.

For operating this system, firstly the electrochemical cell is attached to the elevator mechanism, E. Secondly, an iron crucible, K (19 mm o.d., 16 mm i.d., and 37,5 mm in length) is placed on a steel pedestal, O. The electrical contact to the outer electrode of the zirconia cell is made via this pedestal; 8 g of pure silver, M, is pre-melted within the iron crucible. A 1 to 3 g sample of slag is charged into the iron crucible. These procedures require manual operation. Subsequent steps, however, proceed automatically upon activation of the LCD (liquid crystal display) of a microcomputer:

(1) The iron crucible is moved upward, via an elevator mechanism, P, into a transparent silica reaction tube, H (48 mm o.d., 44 mm i.d., and 238 mm in length).

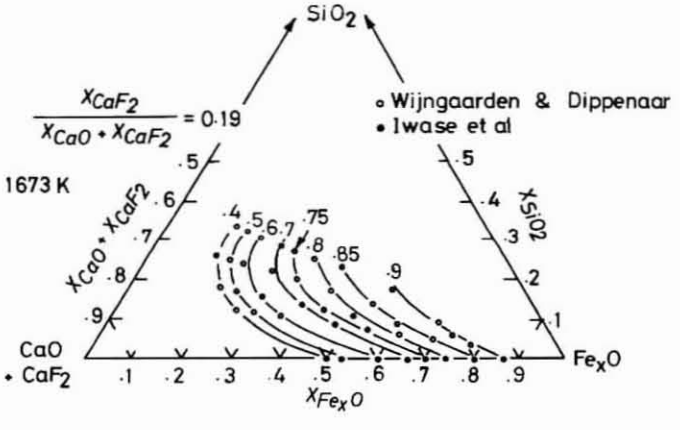

FIGURE 20. Activities of FeO in $CaO + CaF_2 + SiO_2 + FeO$ slags after Van Wijngaarden and Dippenaar[43]

(2) The tube is sealed and flushed with a stream of argon.

(3) By means of an infra-red ray generated by four tungsten filaments, I, the furnace is subsequently heated to the desired temperature, up to 1750 K within 2,5 minutes, by following the computer program.

(4) The furnace temperature is measured with a Pt–PtRh13 thermocouple, N, placed below the iron crucible and monitored on the LCD.

(5) When the temperature reaches the pre-set value, the electrochemical cell is lowered until it contacts both the molten silver and the slag.

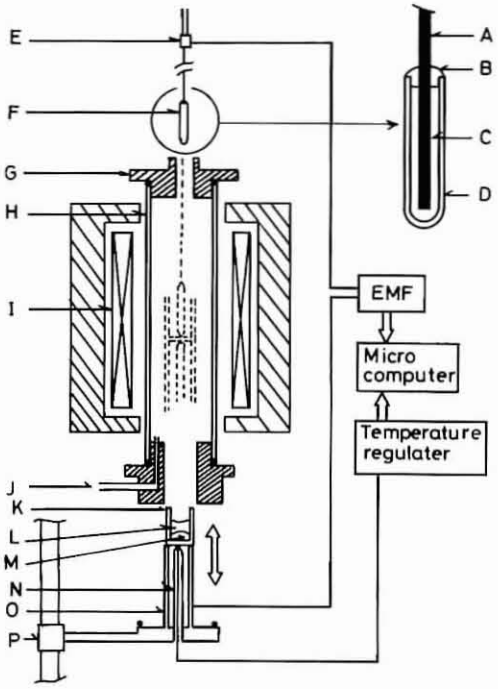

FIGURE 21. Schematic illustration of an automatic activity sensor

A molybdenum rod, B zirconia cement, C Mo + MoO_2 reference electrode, E elevator mechanism, F zirconia cell, G water-cooled brass flange, H silica reaction tube, I tungsten filament, J argon inlet, K iron cricible, M liquid silver, N Pt–PtRh13 thermocouple, O stainless-steel pedestal, P elevator mechanism

(6) Open-circuit cell voltages generated between the molybdenum rod and the steel pedestal are monitored on the LCD of the microcomputer.

(7) After stable emfs (± 0,8 mV) are obtained for at least 1 minute, the electrochemical cell is removed from the iron crucible, which in turn is lowered and discarded in order to prepare for the next activity determination.

(8) The cell potential is then converted to the FeO activity and displayed on the LCD.

In this way, a single activity measurement is completed within 5 minutes.

Figure 22 shows the relationship between a_{FeO} determined by the activity sensor and *(%T.Fe) + (%MnO)* obtained by chemical analysis for industrial slags taken from different ladle shops. As shown in this figure, the empirical parameter *(%T.Fe) + (%MnO)* is proportional to the FeO activities. However, FeO activities taken at one ladle shop were different from those at another, even though the

empirical parameter *(%T.Fe) + (MnO)* was the same. From a thermochemical point of view, this behaviour is quite understandable if the difference in slag basicity is taken into consideration. In other words, the empirical parameter is not an appropriate measure for the control of FeO activity.

The activity sensor can also be applied to laboratory measurements. Figure 23 shows the iso-activity curves for FeO in the system ($CaO + SiO_2 + FeO$) at 1673 K. Moreover, the a_{FeO} data shown in Figure 23 are based on 140 emf measurements, obtained within 35 hours. The application of this facility to elucidate slag–metal reactions in steelmaking processes will be a fruitful area of research in future.

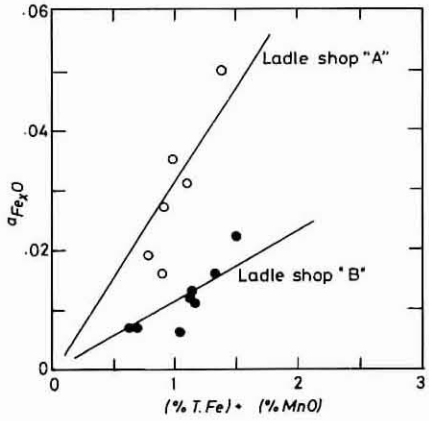

FIGURE 22. Relationship between a_{FeO} determined by the activity sensor and *(%T. Fe) + (%MnO)*(the open and solid circles refer to different ladle shops)

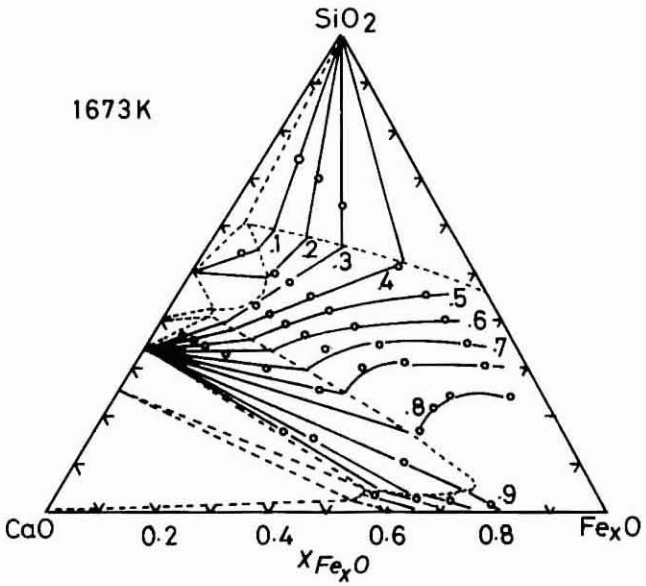

FIGURE 23. Iso-activity curves for FeO in $CaO + SiO_2 + FeO$ slags as determined with the activity sensor

References

1. McLean, A. (1990). Sensor aided process control in iron and steelmaking, *Solid State Ionics*, 40/41, pp. 737-742.
2. Fittere, G.R. (1966). Progress in the development of a device for the direct determination of oxygen in liquid steel, *J. Metals*, 18, August, pp. 961–966.
3. Thomas, J. D. (1976). Oxygen determinations in molten steel by different oxygen probes, *Proc. Nat. Open Hearth Basic Oxygen Steel Conf.* 59, pp. 420–456.
4. Iwase, M. and McLean, A. (1981). Evaluation of electrochemical oxygen probes for use in steelmaking processes, *Solid State Ionics*, 5, pp. 571–574.
5. McLean, A. and Iwase, M. (1983). The importance of oxygen anion diffusion on oxygen activity measurements in liquid steel, *Trans. Iron Steel. Soc. A.I.M.E.*, 2, pp. 45–49.
6. Iwase, M. and Mori, T. (1978). Oxygen permeability of calcia-stabilized zirconia, *Met. Trans.* 9B, pp. 365–370.
7. Iwase, M. and Mori, T. (1978). Oxygen permeability of calcia-stabilized zirconia at low oxygen partial pressures, *Met. Trans.* 9B, pp. 653–656.
8. Schmalzried, H. (1962). Uber Zirkondioxid als Elektrolyte für elektorochemische Untersuchungen bei hoheren Temperaturen, *Elektrochemie*, 66, pp. 572-576. (In German).
9. Pluschkel, W. (1975). Electronic conductivity in the solid electrolyte of oxygen concentration cell, *Arch. Eisenhuttenwes.* 16, pp.11–18.
10. Iwase, M, Tanida, M., McLean, A. and Mori, T. (1981). Electronically driven transport of oxygen from liquid iron to $CO + CO_2$ gas mixtures through calcia-stabilized zirconia, *Met. Trans.*, 12B, pp. 517–524.
11. Iwase, M. and Waseda, Y. (1986). Recent developments in electrochemical oxygen sensors used for iron and steelmaking, *High Temp. Mat. Proc.* 7, pp. 123–131.
12. Swinkels, D. A. J. (1970). Rapid determination of electronic conductivity limits of solid electrolyte, *J. Electrochem.*, pp. 1297–1298.
13. Janke, D. (1982). Oxygen probes based on calcia-doped hafnia or calcium zirconate for use in metallic melts, *Met. Trans.*, 13B, pp. 227–230.
14. Iwase, M., Ichise, E., Takeuchi, M. and Yamasaki, M. (1984). Measurements of the parameter, P_θ, for the determination of mixed ionic *n*-type electronic conduction in commercial zirconia electrolyte, *Trans Japan Inst. Metals*, 25, pp. 43–52.
15. Yamada, K., Murase, M. and Iwase, M. (1986). Determination of mixed ionic and electronic conduction in commercial-grade magnesia-stabilized zirconia electrolyte, *J. Appl. Electrochem.*, 16, pp. 712–718.
16. Wijngaarden, M.J.U.T., Geldenhuis, J. M.A. and Dippenaar, R.J. (1989). A quantitative assessment of mixed ionic and electronic conduction in some commercially available magnesia-stabilized zirconia electrolytes, *Trans. Iron Steel. Soc. AIME.*, 10, pp. 29–38.
17. Cosma, D. and Strathdee, B.A. (1980). The effect of hot metal silicon content on BOF and blast furnace operations, *Steelmaking Proceedings, AIME*, 63, p. 78–81.
18. Nomiyama, H., Ichikawa, H., Marukawa, K., Anezaki, M., and Ueki, H. (1983). Study of optimum silicon content between iron-making and steel-making processes on the hot metal pretreatment, *Tetsu-to-Hagané*, 69, pp. 1738–1746. (In Japanese).
19. Smillie, A. (1982). External treatment of hot metal, *Iron and Steelmaking*, 9, no. 6, pp. 43–45, no. 7, pp. 46–48, no. 8, pp. 33–34, and no. 9, pp. 39–41.

20. Iwase, M., Kim, C.K., McLean, A. and Sommerville, I. D. (1989). In *Modern Steel Processing*, eds. D.H. Samson and D.A.R. Kay, pp. 22–40.
21. Gomyo, M., Sagaguchi, I., Shin-ya, Y. and Iwase, M. (1991). Laboratory and in-plant tests of a solid state silicon sensor incorporating a mixture of ZrO_2 + $ZrSiO_4$ + $Na_2Si_2ZrO_7$ as an auxiliary electrode for rapid determination of silicon levels in blast furnace hot metal, *Iron and Steelmaking*, 13, May, pp. 71-78.
22. Iwase, M. (1988). Rapid determinations of silicon activities in hot metal by means of solid state electrochemical sensors equipped with auxiliary electrode, *Scandinavian J. Metallurgy*, 18, pp. 50–56.
23. Gomyo, K., Sakaguchi, and Iwase, M. (1990). Electrochemical sensors equipped with auxiliary electrode, ZrO_2 + $ZrSiO_4$, *Solid State Ionics*, 40, pp. 770–772.
24. *Phase diagrams for ceramists, 1975 supplement.* (1975). eds. E. M. Levin and H. F. McMurdie, The Amer. Ceram. Soc., Columbus, Ohio, Figure 4533.
25. Raiber, K., Tu, S. W. and Janke, D. (1930). Developments of electrochemical silicon sensor for iron and steel melts, *Steel Research*, 61, pp. 430-437.
26. Iwase, M., Abe, H., and Iritani, H. (1988). Tri-phasic zirconia electrolyte for the determinations of silicon activity in hot metal, *Steel Research*, 59, pp. 433–437.
27. Schakelford, J. F., Nicholson, P. K. and Smeltzer, W. W. (1974). Influence of SiO_2 on sintering of partially stabilized zirconia, *Ceramic Bulletin*, 53, pp. 865–867.
28. Onouye, T., Egami, A., Nishi, S. and Narita, K. (1984). Rapid determination of silicon content in molten iron by silicate electrolyte, *Trans. Iron. Steel. Inst. Japan*, 24, p. B45
29. Ichihara, K., Janke, D. and Engell H.J. (1986). A new silicon sensor for hot metal measurements, *Steel Research*, 57, pp. 166-171.
30. Buiarelli, F., and Granati. P. (1990). New electrochemical probe for silicon determination in hot metal, *Steel Research*, 61, pp. 60–63.
31. Heinz, M. and Janke, D. (1988). Electrochemical sensing of oxygen, chromium and carbon in Fe and NO based melts, *W. I. Philbrook Memorial Symposium Proceedings*, ed. R.J. Fruehan, pp. 205–216. Iron and Steel Soc. AIME, Warrendale, Pa., U.S.A.
32. Fruehan, R.J. (1969). Activities in the liquid Fe–Cr–O system, *Trans. Met. Soc. AIME.*, 245, pp. 1215–1218.
33. Goto, K.S., Sasabe, M., Iguchi, Y., Iwase, M., and Moritani, M. (1990). Collaborative research activities of sensor sub-committee at JSPS. *Solid State Ionics*, 40/41, pp. 758-760.
34. Goto, K. S., Sasabe, M., Iguehi, Y., Iwase, M., and Onouye, T. (1990). Solid state sensor for rapid determination of chromium in molten iron. *Solid State Ionics*, 40/41, pp. 770–772.
35. Iwase, M., Sasabe, M., Iguchi, Y., and Goto, K. S. (1990). Collaborative research activities for the development of electrochemical sensor for rapid determinations of chromium contents in molten iron. *Proc. 6th International Iron and Steel Congress*, 1, pp. 537-542.
36. Geldenhuis, J.M.A. and Dippenaar, R.J. (1990). The evaluation and application of a plug-type oxygen probe in high temperature slag–metal systems at low oxygen potentials. *Proc. 6th International Iron and Steel Congress*, 1, pp. 521–528.
37. Iwase, M. and Kitaguchi, H. (1989) Phase relations of the system ZrO_2 + CaO + P_2O_5 at 1673 K and the electrical conductivity of calcia-stabilized zirconia containing phosphorus pentoxide. *High Temperature Materials and Processes*, 8, pp. 107–110.
38. Iwase, M. and McLean. (1990). *Proc. 6th International Iron and Steel Congress*, 1, pp. 513–520.
39. Taylor, C.R. and Chipman, J. (1942). Equilibria of liquid and simple basic and acidic slags in rotating induction furnace, *Trans. AIME*, 154, pp. 228–247.
40. Iwase, M., Yamada, N., Nishida, K., and Ichise, E. (1981). Rapid determinations of the activities in CaO–FeO liquid slags by disposable electrochemical oxygen sensor. *Trans. ISS/AIME*, 1, pp. 69-75.
41. Iwase, M., Ichise, E., Yamada, N., and Nishida, K. (1984). A thermodynamic study of CaO + CaF_2 + FeO liquid slags used for the external dephosphorization of hot metal. *Ibid.*, 4, pp. 47–53.
42. Van Wijngaarden, M.J.U.T. and Dippenaar, R.J. (1989). The activity of iron oxide in (CaO + CaF_2 + SiO_2 + FeO) slags. *Ibid.*, 10, pp. 11–18.
43. Ogura,T., Fujiwara, R., Mochizuki, R., Kawamoto, K., Oishi, T., and Iwase, M. (1991). Activity determinator for the automatic measurement of the chemical potentials of FeO in metallurgical slags, *Met. Trans.*, submitted for publication.
44. Turkdogan, E.T. (1985). *Making, shaping and treating of steel,* Chapter 13, Association of Iron and Steel Engineers, eds. W.T. Lankfords, N.L. Samway, R.F. Craven and H.F. McGannon,
45. Farrell, J.W., Bilek, P.J., and Hilty, D.C. (1970). *Electric Furnace Proceedings/AIME*, pp. 64–86.
46. *The shrouding of steel flow for casting and teeming* (1986). ed. G. Harry, ISS/AIME, Warrendale, Pa., U.S.A.